Topological Hall effect driven by short-range magnetic order in $EuZn_2As_2$

Enkui Yi,[1,2] Dong Feng Zheng,[3] Feihao Pan,[4] Hongxia Zhang,[4] Bin Wang,[1,2] Bowen Chen,[1,2] Detong Wu,[1,2] Huili Liang,[3] Zeng Xia Mei,[3] Hao Wu,[3] Shengyuan A. Yang,[5] Peng Cheng,[4,*] Meng Wang,[1,†] and Bing Shen[1,2,‡]

[1]*Center for Neutron Science and Technology, Guangdong Provincial Key Laboratory of Magnetoelectric Physics and Devices, School of Physics, Sun Yat-Sen University, Guangzhou, Guangdong 510275, China*
[2]*State Key Laboratory of Optoelectronic Materials and Technologies, Sun Yat-Sen University, Guangzhou, Guangdong 510275, China*
[3]*Songshan Lake Materials Laboratory Dongguan, Guangdong 523808, China*
[4]*Laboratory for Neutron Scattering and Beijing Key Laboratory of Optoelectronic Functional Materials and MicroNano Devices, Department of Physics, Renmin University of China, Beijing 100872, China*
[5]*Research Laboratory for Quantum Materials, Singapore University of Technology and Design, Singapore 487372, Singapore*

(Received 10 December 2022; accepted 18 January 2023; published 24 January 2023; corrected 18 September 2023)

Short-range (SR) magnetic orders such as magnetic glass orders or fluctuations in a quantum system usually host exotic states or critical behaviors. Like the long-range (LR) magnetic orders, SR magnetic orders can also break time-reversal symmetry and drive the nonzero Berry curvature leading to novel transport properties. In this work, we report that in $EuZn_2As_2$ compound, besides the LR *A*-type antiferromagnetic (AF) order, the SR magnetic order is observed in a wide temperature region. Magnetization measurements and electron spin resonance (ESR) measurements reveal the ferromagnetic (FM) correlations for this SR magnetic order which results in an obvious anomalous Hall effect above the AF transition. Moreover the ESR results reveal that this FM SR order coexists with LR AF order exhibiting anisotropic magnetic correlations below the AF transition. The interactions of LR and SR magnetism evolving with temperature and field can host nonzero spin chirality and berry curvature leading to additional topological Hall contribution even in a centrosymmetric simple AF system. Our results indicate that $EuZn_2As_2$ is a fertile platform to investigate exotic magnetic and electronic states.

DOI: 10.1103/PhysRevB.107.035142

Short-range (SR) magnetic orders are widely investigated and draw great interest in various quantum systems in condensed matter physics. Compared to long-range (LR) magnetic orders, SR magnetic orders such as magnetic glass orders (static) or magnetic fluctuations (dynamic), etc., can emerge at temperatures much higher than those for the establishment of LR magnetic orders, accompanied with exotic orders such as unconventional superconducting order, electron nematic order, etc., hosting critical behaviors and novel quantum phenomena [1,2]. For a topological system, the LR magnetic orders are usually considered to develop magnetic nontrivial topological states due to robust magnetism and large magnetic gaps. Recently, the observed SR magnetic orders in topological materials such as $EuCd_2As_2$ and $MnBi_2Te_4$ also drive magnetic nontrivial topological states and host abnormal transport behaviors above the antiferromagnetic (AF) transition due to time-reversal symmetry breaking [3–7]. This prompts us to consider SR magnetic orders such as magnetic fluctuations, which have been overlooked for a long time in topological systems, to design magnetic nontrivial topological states or achieve the topological effects in the high-temperature (or even room-temperature) region [8,9].

In Eu-122 systems, such as $EuCd_2As_2$, $EuSn_2As_2$, or $EuIn_2As_2$, besides the AF transition at low temperatures (T_{AF}), SR magnetic orders were observed in a wide temperature region [4,6,10–15]. For example, in $EuCd_2As_2$, strong spin fluctuations emerge around 100 K and drive the magnetic Weyl Fermions far above the AF transition [4]. Correspondingly, unconventional anomalous Hall and Nernst effects also emerge above T_{AF} and have different temperature and field evolutions than those below T_{AF} [5]. In $EuIn_2As_2$ (considered as an axion insulator), a magnetic polaron (MP) is revealed above T_{AF} leading to large negative magnetoresistivity (MR) [14]. In addition, helical magnetic orders accompanied with *A*-type AF lattice below T_{AF} were also observed in some research indicating complicate magnetic structure for $EuIn_2As_2$ [12]. Eu-122 compounds provide a fertile playground for investigating the interplay between various magnetism and electron topologies hosting novel transport properties. Different from metallic $EuCd_2As_2$ or $EuIn_2As_2$, $EuZn_2As_2$ is a semiconducting compound but shares a similar crystal structure. Although the simple AF transition is observed, the transport features above this transition may suggest the presence of complicated magnetic orders and interactions which are still poorly understood [16–18]. In this work, we perform a systematic study of semiconducting $EuZn_2As_2$. An in-plane AF structure is identified by our single-crystal

*pcheng@ruc.edu.cn
†wangmeng5@mail.sysu.edu.cn
‡shenbing@mail.sysu.edu.cn

neutron scattering measurements around $T_{AF} = 20$ K. Besides this LR magnetic order, the SR ferromagnetic (FM) order is revealed by electron spin resonance (ESR) and magnetization measurements. This SR FM order spans a wide temperature region even above T_{AF} and drives the anomalous Hall effect (AHE). More interestingly, the prominent topological Hall effect (THE) is observed in a centrosymmetric system in the absence of helical magnetic orders. With temperature decreasing to 12 K, the THE exhibits a small shoulder due to the change of the interaction between LR AF and SR FM orders. These abnormal behaviors suggest that the complicated interaction of LR and SR in $EuZn_2As_2$ can drive large Berry curvature and nonzero spin chirality hosting multiple novel transport properties.

Single crystals of $EuZn_2As_2$ were grown by the Sn-flux method [16–18]. Structure and elemental composition of crystals were assessed using x-ray diffraction and energy dispersive x-ray spectroscopy respectively. A single-crystal neutron diffraction experiment was carried out on the Xingzhi cold neutron triple-axis spectrometer at the China Advanced Research Reactor (CARR) [19]. A single crystal with the mass of 0.1 g was aligned to the (HHL) scattering plane. The incident neutron energy was fixed at 15 meV with a neutron velocity selector used upstream to remove higher-order neutrons. Transport measurements were performed on a commercial physical property measurement system (PPMS Dynacool, Quantum Design). Magnetization measurements were carried on a vibrating sample magnetometer (VSM) based on the PPMS. ESR signals were obtained by a Bruker EMX plus X-band (9.365 GHz) CWEPR spectrometer.

As shown in Fig. 1(a), $EuZn_2As_2$ exhibits semiconducting behavior revealed by the temperature dependent resistivity $[\rho_{xx}(T)]$, in sharp contrast to metallic $EuCd_2As_2$ or $EuIn_2As_2$ [14,20,21]. An abnormal peak was observed around 20 K both in $\rho_{xx}(T)$ and temperature dependent magnetization $[M(T)]$ due to a magnetic transition shown in Fig. 1(b). To check this transition and related magnetic order, single-crystal neutron diffraction measurements were performed and the scans along the $(00L)$ reciprocal-lattice direction are shown in Fig. 1(c). The magnetic Bragg peaks at $L = 0.5n$ (n = odd number) are observed at 3.5 K but absent at 60 K. Besides, the magnetic Bragg peaks indexed by $(11L)$ with $L = 0.5n$ (n = odd number) were also identified. After carefully checking diffraction results for several other directions, we did not observe additional incommensurate magnetic Bragg peaks such as those in $EuIn_2As_2$ [12]. The neutron diffraction results support an A-type spin configuration with moments lying in the ab plane below transition temperature T_{AF} without the appearance of complex helical magnetic structure consistent with a previous report [12] shown in Fig. 1(e). The temperature dependent intensity of magnetic Bragg peak (0,0,2.5) is shown in Fig. 1(d). The peak intensity quickly drops to background value at a transition temperature (T_{AF}), indicating that the long-range antiferromagnetic order vanishes above T_{AF}, consistent with the magnetization measurements results.

The field dependent longitudinal resistivity $[\rho_{xx}(\mu_0 H)]$ and Hall resistivity $[\rho_{xy}(\mu_0 H)]$ exhibit systematical temperature evolution as shown in Figs. 3(a) and 3(b). Prominent negative MR is observed at low temperatures. With increasing temperature, this prominent negative MR becomes weak gradually but can persist up to a temperature (around 100 K) far above T_{AF}. Correspondingly, $\rho_{xy}(\mu_0 H)$ exhibits nonlinear field dependence below 100 K indicating the presence of an extra Hall contribution (AHE) from the magnetism or nonzero Berry curvature. With further decrease in temperature (below 30 K), after subtracting the normal Hall contribution due to the Lorentz force with the linear field response, a discrepancy between $\rho_{xy}(\mu_0 H)$ and $M(\mu_0 H)$ is observed, suggesting the emergence of an additional Hall contribution (THE) besides AHE. Thus, the total Hall resistivity for $EuZn_2As_2$ can be expressed as [22,23]

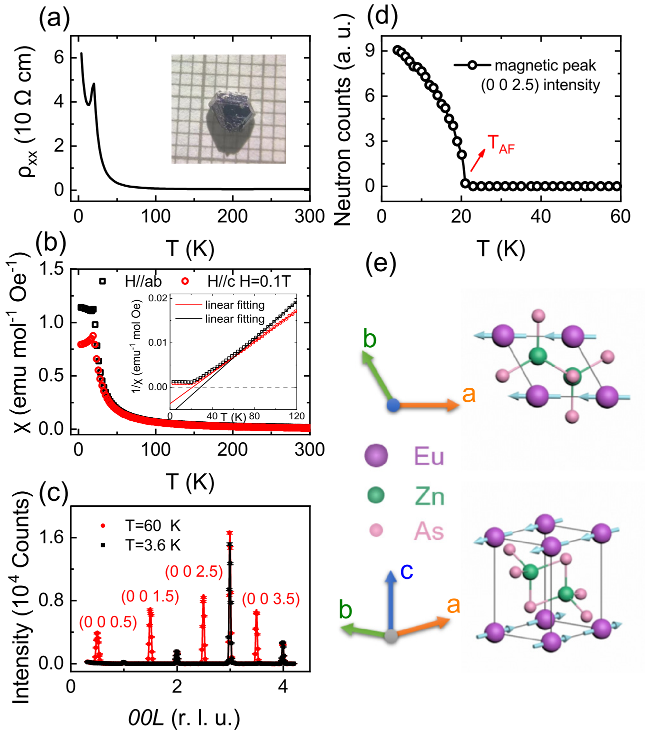

FIG. 1. (a) Temperature dependent longitudinal resistivity $\rho_{xx}(T)$. (b) Temperature dependence of magnetic susceptibilities $[\chi(T)]$ with the applied field of 0.1 T perpendicular ($\mu_0 H \parallel ab$) and parallel ($\mu_0 H \parallel c$) to the c axis of the crystal respectively. The inset: the inverses of magnetic susceptibilities for $\mu_0 H \parallel ab$ and $\mu_0 H \parallel c$ fitted by the Curie-Weiss law. (c) Neutron diffraction scans along the $(00L)$ reciprocal-lattice direction for 3.6 and 60 K. (d) The neutron intensity of magnetic peak (0 0 2.5) as a function of temperature. (e) The schematic crystal and magnetic structure of $EuZn_2As_2$ below T_{AF}.

$$\rho_{xy} = \rho_{xy}^N + \rho_{xy}^A + \rho_{xy}^T = R_0\mu_0 H + AM + \rho_{xy}^T, \quad (1)$$

where ρ_{xy}^N, ρ_{xy}^A, and ρ_{xy}^T are the normal Hall resistivity, anomalous Hall resistivity, and topological Hall resistivity respectively, while R_0 and A are the Hall coefficient and the anomalous Hall coefficient. According to this formula and the data of $M(\mu_0 H)$, ρ_{xy}^A and ρ_{xy}^T are separated from ρ_{xy} and presented in Figs. 2(c) and 2(d).

The first interesting observation is the prominent AHE spanning a large temperature region even with the absence of AF order. For an AF system, it is usually surprising to host obvious AHE due to the absence of net magnetization.

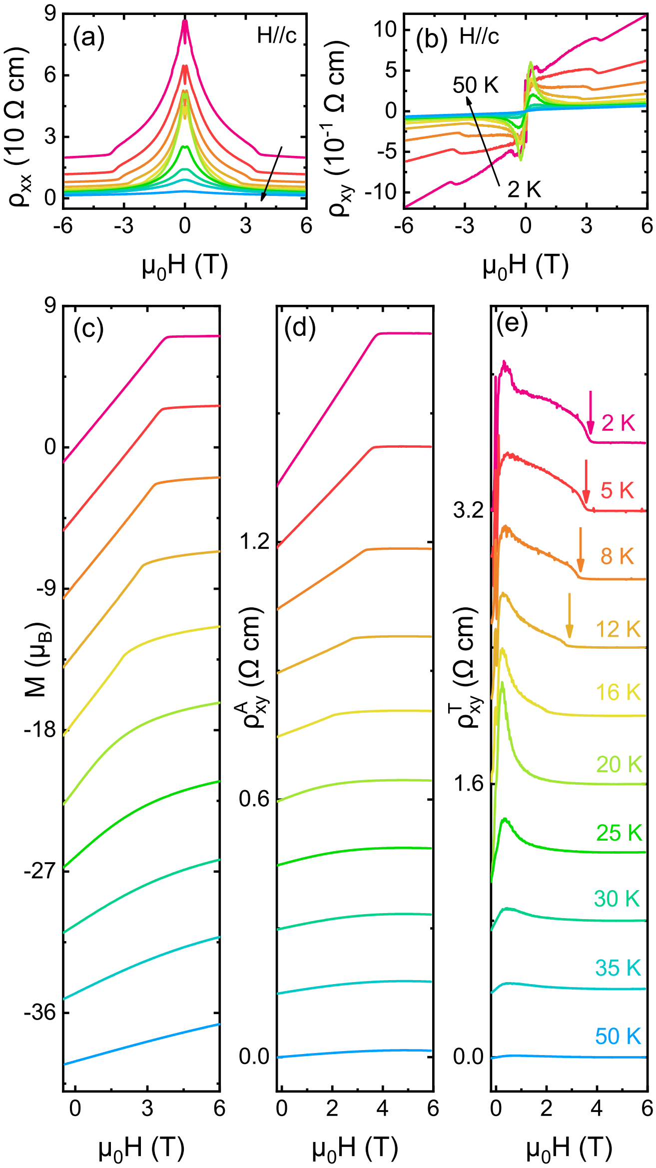

FIG. 2. The field dependent longitudinal resistivity $\rho_{xx}(\mu_0 H)$ (a), and Hall resistivity $\rho_{xy}(\mu_0 H)$ (b) at 2, 5, 8, 12, 16, 20, 25, 30, 35, and 50 K. According to the formula $\rho_{xy} = \rho^N_{xy} + \rho^A_{xy} + \rho^T_{xy} = R_0\mu_0 H + AM + \rho^T_{xy}$, the AHE component ρ^A_{xy} and THE component ρ^T_{xy} are extracted from the total Hall resistivity ρ_{xy}. The field dependent magnetization $M(\mu_0 H)$ (c), anomalous Hall resistivity $\rho^A_{xy}(\mu_0 H)$ (d), and topological Hall resistivity $\rho^T_{xy}(\mu_0 H)$ (e) at 2, 5, 8, 12, 16, 20, 25, 30, 35, and 50 K. The absolute values of $M(\mu_0 H)$, $\rho^A_{xy}(\mu_0 H)$, and $\rho^T_{xy}(\mu_0 H)$ shift at various temperatures. In $\rho^T_{xy}(\mu_0 H)$ curves, the second-shoulder features are marked by arrows.

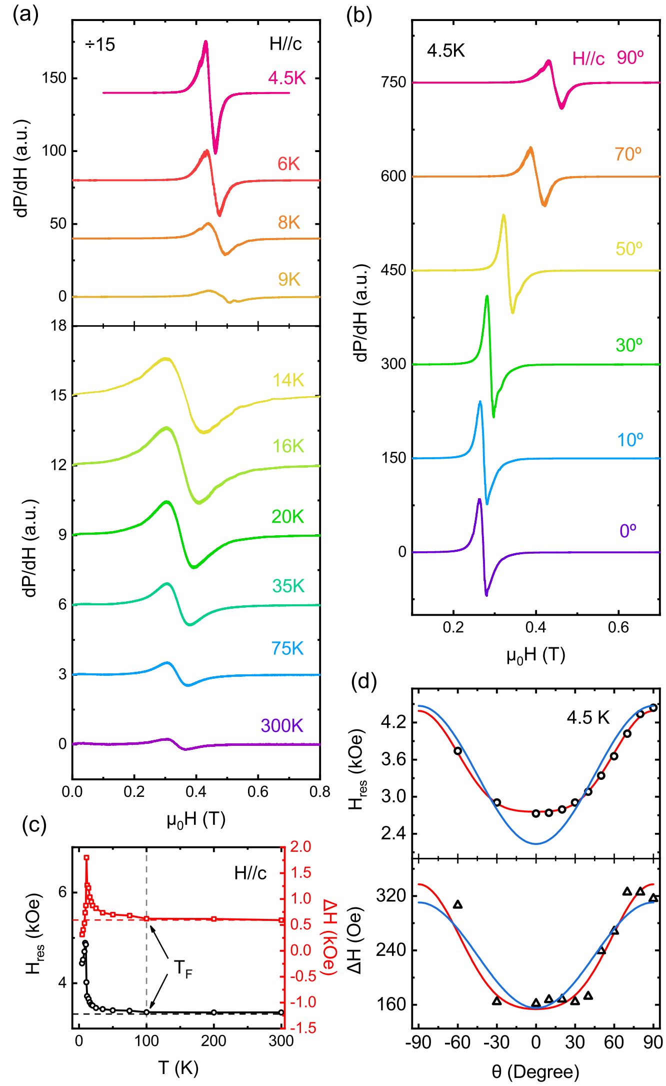

FIG. 3. (a) ESR spectra of $EuZn_2As_2$ at 4.5, 6, 8, 9, 14, 16, 20, 35, 75, and 300 K with the applied field along the *c* axis. (b) ESR spectra of $EuZn_2As_2$ with θ from 0° to 90°, where θ is the angle between the applied field and the *ab* plane of the crystal. (c) Temperature dependence of resonance field $H_{res}(\theta)$ (left) and line width ΔH (right). (d) Angular dependence of H_{res} (θ) (upper) and $\Delta H(\theta)$ (lower) at 4.5 K. Red lines represent the fitting curves for $H_{res}(\theta)$ and $\Delta H(\theta)$ by formulas as $H_{res} = a_1\{1 + \sin^2(\theta) + a_2[3\cos^2(\theta) - 1]^2\}$ and $\Delta H = a_1\{1 + \sin^2(\theta) + a_2[3\sin^2(\theta) - 1]^2\}$ respectively, where a_1 and a_2 are fitting coefficients. The blue line can be expressed as $H_{res} = a_1[1 + \sin^2(\theta)]$ and $\Delta H = a_1[1 + \sin^2(\theta)]$ [27].

But recent experimental researches revealed that the chiral magnetic structure or Berry curvature could also host large AHE based on an AF structure [24–26]. For $EuZn_2As_2$, only a simple collinear AF order is identified by our measurements, in contrast to $EuCd_2As_2$ or $EuIn_2As_2$ which hosts an additional helical magnetic order besides the basic collinear AF structure [12]. Such simple magnetic structure in $EuZn_2As_2$ seems unable to host large net magnetization, indicating a possible different origin for the large AHE. Another observed abnormal transport feature is the prominent THE. At low temperatures, it exhibits a two-peak feature [a peak around zero field with a small shoulder in a larger field region marked by arrows in Fig. 2(e)]. With increasing temperature, the small shoulder become weak gradually and is eventually invisible at 12 K. In addition, THE can also persist to the temperature region above T_{AF} where the AF LR magnetic order vanishes. Usually THE is considered to originate from the movement of skyrmions in noncentrosymmetric noncollinear magnets hosting the nonzero scalar spin chirality [23]. However, these physics pictures cannot describe the case of $EuZn_2As_2$ with a simple colinear AF magnetic structure and a centrosymmetric crystal structure.

To understand these AHE and THE, short-range magnetic order, which may be overlooked for a topologically protected system, needs to be considered in $EuZn_2As_2$. It is observed that the $M(\mu_0 H)$ curves for both $\mu_0 H \parallel ab$ and $\mu_0 H \parallel c$ start to deviate from the Curie-Weiss behavior at a temperature T_F (around 100 K) much higher than T_{AF} coinciding with the presence of negative MR. These abnormal transport behaviors reveal large-scale SR magnetic interactions before the establishment of the LR AF orders. To further investigate this SR order, ESR measurements were performed in a wide temperature region as shown in Fig. 3. All ESR spectra [(dP/dH) vs H] exhibit a single exchange-narrowed resonance without other hyperfine lines, as shown in Figs. 3(a) and 3(b). At high temperatures, the ESR signals exhibit an asymmetric Dysonian shape which is characteristic of localized magnetic moments in a lattice with a skin depth for a single crystal [7,28,29]. With decreasing temperature, the ESR signals become stronger and deviate from the Dysonian-shape relation gradually. It is observed that the ESR line width ΔH exhibits weak temperature dependence above T_F (100 K), consistent with keeping the resonant field $H_{\rm res}$ at 3350 Oe, associated with the g factor ($g = h\nu/\mu_0 H_{\rm res}$, where ν is electromagnetic wave frequency) of 1.99 in the same temperature region where localized Eu^{2+} $4f$ electron spins dominate this paramagnetic state [30,31]. Below T_F, ΔH starts to increase while $H_{\rm res}$ decreases with decreasing temperature above T_{AF}. These behaviors reveal that an effective internal magnetic field develops as the magnetic correlations occur with cooling the system down to T_F. And it is noticed that T_F is roughly five times larger than T_{AF}, which indicates magnetic interactions drive SR magnetic order over a large temperature scale above T_{AF}.

Below T_{AF} for $H \parallel ab$, $H_{\rm res}$ increases to the value of 2728 Oe at 4.5 K associated with the increase of $M(T)$ during the cooling process, which is consistent with positive Curie-Weiss temperature of $\Theta = 25$ K acquired by fitting $M(T)$ curves. These behaviors reveal a FM correlation for in-plane magnetic interactions favoring the A-type AF structure revealed by our neutron results. In contrast, for $H \parallel c$, $H_{\rm res}$ drops sharply with decreasing temperature below T_{AF} and to 1510 at 4.5 K, consistent with the decrease of $M(T)$, suggesting the AFM correlation for interplane magnetic interactions. But the $\Theta = 20$ K value acquired by fitting $M(T)$ curves for $H \parallel c$ reveals that the FM correlation still persists, accompanied by an A-type AF order. As shown in Fig. 3(d), the angular ESR line width $\Delta H(\theta)$ and resonant field $H_{\rm res}(\theta)$ (where θ is the angle between the applied field and the ab plane) reveal the anisotropic magnetic correlations. In a weakly correlated spin system such as a paramagnetic (PM) or weakly correlated AF system, $H_{\rm res}(\theta)$ and $\Delta H(\theta)$ follow the relations $H_{\rm res}(\theta) \sim [\sin^2(\theta) + 1]$ and $\Delta H(\theta) \sim [\cos^2(\theta) + 1]$ respectively. These angular dependent laws can well describe the anisotropy due to the interactions for uncorrelated spins such as that for the type-A AF state in $MnBi_2Te_4$ or for the PM state in intrinsically low-dimensional van der Waals magnets [7,27]. Here our angular data violate these relations, suggesting stronger and more anisotropic magnetic

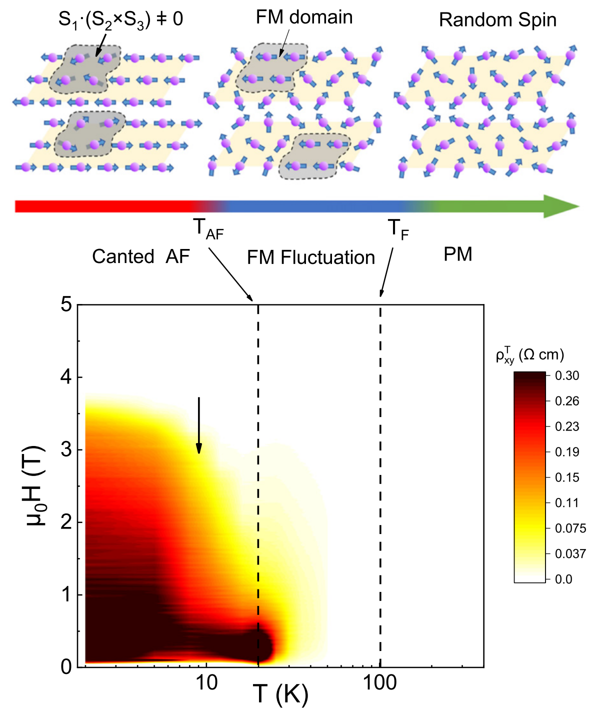

FIG. 4. The phase diagram for $EuZn_2As_2$. Top: The schematic of various magnetic states in different temperature regions. The canted AF state can host local nonzero spin chirality. FM fluctuations can host local FM domains. For paramagnetic (PM) state the spins are random and isotropic. Bottom: The color plot for topological Hall resistivity. The black broken lines divide the diagram into three regions. The arrow around 12 K indicates the vanishing of the second shoulder for THE.

correlations. It is observed that our $\Delta H(\theta)$ and $H_{\rm res}(\theta)$ follow the relations $H_{\rm res} = a_1\{1 + \sin^2(\theta) + a_2[3\cos^2(\theta) - 1]^2\}$ and $\Delta H = a_1\{1 + \sin^2(\theta) + a_2[3\sin^2(\theta) - 1]^2\}$ respectively (where a_1 and a_2 are fitting coefficients), which describe typical two-dimensional magnetic systems with the increasing dominance of long-wavelength fluctuations such as the FM state in $Cr_2Ge_2Te_6$ [27]. These anisotropic magnetization and ESR results suggest the following: (1) For $EuZn_2As_2$ with layered crystal structure, the in-plane FM interactions are expected to be much stronger than the interlayer AFM interactions. (2) the FM correlation spans a large temperature scale for both in-plane and out-of-plane directions [4]. (3) The substantial frustrations which may be due to nearest and next-nearest neighbor magnetic exchange couplings drive an anisotropic SR FM order strongly interacting with the static LR AFM order. These SR magnetic orders may be also sensitive to the applied field and undergo an evolution for spin freezing with an anisotropic dynamic behavior, which need further study by magnetic dynamic spectrum measurements with applied fields.

Figure 4 shows the phase diagram of $EuZn_2As_2$. In a frustrated system, upon cooling the system from the PM state, the in-plane FM correlations increase and the dipolar interactions will then further stabilize FM correlations out of the plane. The related SR FM order divides the system into local FM domains whose net magnetization brings the additional AHE term for ρ_{xy} below T_F. Upon further decreasing the temperature, both dipolar and AFM interlayer exchange interactions prefer magnetization changes from an out-of-plane to an in-plane orientation leading to an *A*-type AFM structure. However, the FM SR order still persists and interacts with the established long-range order, leading to a canted AF structure. These canted spins with local FM orders can also host nonzero spin chirality in a centrosymmetric system such as that in $EuCd_2As_2$, leading to the additional THE contribution which can even persist above T_{AF} [5,21,32]. For a time, the SR magnetic orders were overlooked in developing a robust magnetic topological system. But the recent studies in Mn-Bi-Te and Eu-122 systems revealed that the SR magnetic orders [33], such as magnetic fluctuations or magnetic polarons, can also change the topological nature of a magnetic system, e.g., the SR magnetic orders may drive novel features at higher temperatures such as the observed magnetic Weyl point far above T_{AF} [4,7,14]. For $EuZn_2As_2$, when the magnetic correlations become strong enough, the system can also change the local magnetic chirality and Berry curvature, probably mediated by the magnetic fluctuations hosting the novel transport properties. Moreover, it is observed that THE exhibits a second shoulder feature below 12 K, which may suggest a crossover by the competing interaction of the LR AF order and the SR FM order. In $EuZn_2As_2$, due to the evolved magnetic correlations the SR magnetic order can persist and interact with electron and LR magnetic order on a wide scale, resulting in various abnormal transport features.

In summary, we systemically investigate the magnetism and the related transport properties for $EuZn_2As_2$. The SR FM order is revealed prominently in a temperature region above the AF transition. This short-range order results in a large AHE above T_{AF} and canted AF orders below T_{AF}. These interacting magnetic orders drive THE in a centrosymmetric system. Our results indicate the short-range magnetic order can bring about nonzero spin chirality and the Berry curvature, driving novel transport properties which should be also considered and emphasized for the investigation of the interplay between magnetism and topology in quantum materials.

This work was supported by Guangzhou Basic and Applied Basic Research Foundation (Grant No. 202201011798); Guangdong Basic and Applied Basic Research Foundation (Grants No. 2022A1515010035 and No. 2021B1515120015); the Open Research Fund of Songshan Lake Materials Laboratory 2021SLABFN11, OEMT-2021-PZ-02; National Natural Science Foundation of China (NSFC) (Grants No. U2130101, No. 12174454, No. 92165204, No. U2030106, and No. 12074426); National Key Research and Development Program of China (Grant No. 2019YFA0705702); Physical Research Platform (PRP) in School of Physics, Guangdong Provincial Key Laboratory of Magnetoelectric Physics and Devices (LaMPad), Sun Yat-sen University.

[1] H. von Lohneysen, A. Rosch, M. Vojta, and P. Wölfle, Fermi-liquid instabilities at magnetic quantum phase transition, Rev. Mod. Phys. **79**, 1015 (2007).

[2] S. A. Kivelson, I. P. Bindloss, E. Fradkin, V. Oganesyan, J. M. Tranquada, A. Kapitulnik, and C. Howald, How to detect fluctuating stripes in the high-temperature superconductors, Rev. Mod. Phys. **75**, 1201 (2003).

[3] X. Y. Cao, J. X. Yu, P. L. Leng, C. J. Yi, X. Y. Chen, Y. K. Yang, S. S. Liu, L. Y. Kong, Z. H. Li, X. Dong, Y. G. Shi, M. Bibes, R. Peng, J. D. Zang, and F. X. Xiu, Giant nonlinear anomalous Hall effect induced by spin-dependent band structure evolution, Phys. Rev. Res. **4**, 023100 (2022).

[4] J. Z. Ma, S. M. Nie, C. J. Yi, J. Jandke, T. Shang, M. Y. Yao, M. Naamneh, L. Q. Yan, Y. Sun, A. Chikina, V. N. Strocov, M. Medarde, M. Song, Y. M. Xiong, G. Xu, W. Wulfhekel, J. Mesot, M. Reticcioli, C. Franchini, C. Mudry, M. Muller, Y. G. Shi, T. Qian, H. Ding, and M. Shi, Spin fluctuation induced Weyl semimetal state in the paramagnetic phase of $EuCd_2As_2$, Sci. Adv. **5**, eaaw4718 (2019).

[5] Y. Xu, L. Das, J. Z. Ma, C. J. Yi, S. M. Nie, Y. G. Shi, A. Tiwari, S. S. Tsirkin, T. Neupert, M. Medarde, M. Shi, J. Chang, and T. Shang, Unconventional Transverse Transport above and lelow the Magnetic Transition Temperature in Weyl Semimetal $EuCd_2As_2$, Phys. Rev. Lett. **126**, 076602 (2021).

[6] M. C. Rahn, J. R. Soh, S. Francoual, L. S. I. Veiga, J. Strempfer, J. Mardegan, D. Y. Yan, Y. F. Guo, Y. G. Shi, and A. T. Boothroyd, Coupling of magnetic order and charge transport in the candidate Dirac semimetal $EuCd_2As_2$, Phys. Rev. B **97**, 214422 (2018).

[7] A. Alfonsov, J. I. Facio, K. Mehlawat, A. G. Moghaddam, R. Ray, A. Zeugner, M. Richter, J. van den Brink, A. Isaeva, B. Buchner, and V. Kataev, Strongly anisotropic spin dynamics in magnetic topological insulator, Phys. Rev. B **103**, L180403 (2021).

[8] J. Ge, Y. Z. Liu, J. H. Li, H. Li, T. C. Luo, Y. Wu, Y. Xu, and J. Wang, High-Chern-number and high-temperature quantum Hall effect without Landau level, Nat. Sci. Rev. **7**, 1280 (2020).

[9] N. J. Ghimire, R. L. Dally, L. Poudel, D. C. Jones, D. Michel, N. T. Magar, M. Bleuel, M. A. McGuire, J. S. Jiang, J. F. Mitchell, J. W. Lynn, and I. Mazin, Competing magnetic phases and fluctuation-driven scalar spin chirality in the kagome metal YMn_6Sn_6, Sci. Adv. **6**, eabe2680 (2020).

[10] N. H. Jo, B. Kuthanazhi, Y. Wu, E. Timmons, T. H. Kim, L. Zhou, L. L. Wang, B. G. Ueland, A. Palasyuk, D. H. Ryan, R. J. McQueeney, K. Lee, B. Schrunk, A. A. Burkov, R. Prozorov, S. L. Bud'ko, A. Kaminski, and P. C. Canfield, Competing magnetic phases and fluctuation-driven scalar spin chirality in the kagome metal YMn_6Sn_6, Phys. Rev. B **101**, 140402(R) (2020).

[11] K. M. Taddei, L. Yin, L. D. Sanjeewa, Y. Li, J. Xing, C. dela Cruz, D. Phelan, A. S. Sefat, and D. S. Parker, Single pair of Weyl nodes in the spin-canted structure of $EuCd_2As_2$, Phys. Rev. B **105**, L140401 (2022).

[12] S. X. M. Riberolles, T. V. Trevisan, B. Kuthanazhi, T. W. Heitmann, F. Ye, D. C. Johnston, S. L. Bud'ko, D. H. Ryan, P. C. Canfield, A. Kreyssig, A. Vishwanath, R. J. McQueeney, L. L. Wang, P. P. Orth, and B. G. Ueland, Magnetic crystalline-symmetry-protected axion electrodynamics and field-tunable unpinned Dirac cones in $EuIn_2As_2$, Nat. Commun. **12**, 999 (2021).

[13] Yi En-Kui, Wang Bin, Shen Han, and Shen Bing, Properties of axion insulator candidate layered $Eu_{1-x}Ca_xIn_2As_2$, Acta Phys. Sin. **70**, 127502 (2021).

[14] Y. Zhang, K. Deng, X. Zhang, M. Wang, Y. Wang, C. Liu, J. W. Mei, S. Kumar, E. F. Schwier, K. Shimada, C. Y. Chen, and B. Shen, In-plane antiferromagnetic moments and magnetic polaron in the axion topological insulator candidate $EuIn_2As_2$, Phys. Rev. B **101**, 205126 (2020).

[15] H. Sun, C. Chen, Y. Hou, W. Wang, Y. Gong, M. Huo, L. Li, J. Yu, W. Cai, N. Liu, R. Wu, D.-X. Yao, and M. Wang, Magnetism variation of the compressed antiferromagnetic topological insulator $EuSn_2As_2$, Sci China Phys., Mech. Astron. **64**, 118211 (2021).

[16] Z. C. Wang, E. Been, J. Gaudet, G. M. A. Alqasseri, K. Fruhling, X. Yao, U. Stuhr, Q. Zhu, Z. Ren, Y. Cui, C. Jia, B. Moritz, S. Chowdhury, T. Devereaux, and F. Tafti, Anisotropy of the magnetic and transport properties of $EuZn_2As_2$, Phys. Rev. B **105**, 165122 (2022).

[17] J. Blawat, M. Marshall, J. Singleton, E. X. Feng, H. B. Cao, W. W. Xie, and R. Y. Jin, Unusual electrical and magnetic properties in layered $EuZn_2As_2$, Adv. Quantum Technol. **5**, 2200012 (2022).

[18] Z. Bukowski, D. Rybicki, M. Babij, J. Przewoznik, L. Gondek, J. Zukrowski, and C. Kapusta, Canted antiferromagnetic order in $EuZn_2As_2$ single crystals, Sci. Rep. **12**, 14718 (2022).

[19] P. Cheng, H. X. Zhang, W. Bao, A. Schneidewind, P. Link, A. T. D. Grunwald, R. Georgii, L. J. Hao, and Y. T. Liu, Design of the cold neutron triple-axis spectrometer at the china advanced research reactor, Nucl. Instrum. Methods Phys. Res., Sect. A **821**, 17 (2016).

[20] C. W. Niu, N. Mao, X. T. Hu, B. B. Huang, and Y. Dai, Quantum anomalous Hall effect and gate-controllable topological phase transition in layered $EuCd_2As_2$, Phys. Rev. B **99**, 235119 (2019).

[21] J. R. Soh, F. de Juan, M. G. Vergniory, N. B. M. Schroter, M. C. Rahn, D. Y. Yan, J. Jiang, M. Bristow, P. Reiss, J. N. Blandy, Y. F. Guo, Y. G. Shi, T. K. Kim, A. McCollam, S. H. Simon, Y. Chen, A. I. Coldea, and A. T. Boothroyd, Ideal Weyl semimetal induced by magnetic exchange, Phys. Rev. B **100**, 201102(R) (2019).

[22] B. Wang, E. K. Yi, L. Y. Li, J. W. Qin, B. F. Hu, B. Shen, and M. Wang, Magnetotransport properties of the kagome magnet $TmMn_6Sn_6$, Phys. Rev. B **106**, 125107 (2022).

[23] N. Nagaosa, J. Sinova, S. Onoda, A. H. MacDonald, and N. P. Ong, Anomalous Hall effect, Rev. Mod. Phys. **82**, 1539 (2010).

[24] Y. J. Deng, Y. J. Yu, M. Z. Shi, Z. X. Guo, Z. H. Xu, J. Wang, X. H. Chen, and Y. B. Zhang, Quantum anomalous Hall effect in intrinsic magnetic topological insulator $MnBi_2Te_4$, Science **367**, 895 (2020).

[25] C. Liu, Y. C. Wang, H. Li, Y. Wu, Y. X. Li, J. H. Li, K. He, Y. Xu, J. S. Zhang, and Y. Y. Wang, Robust axion insulator and Chern insulator phases in a two-dimensional antiferromagnetic topological insulator, Nat. Mater. **19**, 522 (2020).

[26] S. Nakatsuji, N. Kiyohara, and T. Higo, Large anomalous Hall effect in a non-collinear antiferromagnet at room temperature, Nature (London) **527**, 212 (2015).

[27] J. Zeisner, A. Alfonsov, S. Selter, S. Aswartham, M. P. Ghimire, M. Richter, J. van den Brink, B. Buchner, and V. Kataev, Magnetic anisotropy and spin-polarized two-dimensional electron gas in the van der Waals ferromagnet $Cr_2Ge_2Te_6$, Phys. Rev. B **99**, 165109 (2019).

[28] G. Feher and A. F. Kip, Electron spin resonance absorption in metals. I. Experimental, Phys. Rev. **98**, 337 (1955).

[29] F. J. Dyson, Electron spin resonance absorption in metals. II. Theory of electron diffusion and the skin effect, Phys. Rev. **98**, 349 (1955).

[30] Y. V. Goryunov, A. V. Levchenko, and A. N. Nateprov, Unusual magnetism of the Eu based compounds $EuB_{6-x}C_x$, $EuZn_2As_2$: the low temperature ESR study, J. Phys.: Conf. Ser. **400**, 032013 (2012).

[31] Y. Goryunov, V. Fritsch, H. V. Lohneysen, and A. Nateprov, The ESR study of Eu ternary pnictides $EuCd_2Sb_2$, $EuZn_2As_2$, J. Phys. Conf. Ser. **391**, 012015 (2012).

[32] L. L. Wang, N. H. Jo, B. Kuthanazhi, Y. Wu, R. J. McQueeney, A. Kaminski, and P. C. Canfield, Single pair of Weyl fermions in the half-metallic semimetal $EuCd_2As_2$, Phys. Rev. B **99**, 245147 (2019).

[33] S. H. Lee, Y. Zhu, Y. Wang, L. Miao, T. Pillsbury, H. Yi, S. Kempinger, J. Hu, C. A. Heikes, P. Quarterman, W. Ratcliff, J. A. Borchers, H. Zhang, X. Ke, D. Graf, N. Alem, C. Z. Chang, N. Samarth, and Z. Mao, Spin scattering and noncollinear spin structure-induced intrinsic anomalous Hall effect in antiferromagnetic topological insulator $MnBi_2Te_4$, Phys. Rev. Res. **1**, 012011(R) (2019).

Correction: A grant number in the Acknowledgments contained an error and has been fixed.